DOI: 10.1002/chem.200902110

A Combined Theoretical and Experimental Investigation on the Enantioselective Oxidation of Aryl Benzyl Sulfides in the Presence of a Chiral Titanium Catalyst

Francesco Naso,[a] Maria Annunziata M. Capozzi,[b] Andrea Bottoni,*[c] Matteo Calvaresi,[c] Valerio Bertolasi,[d] Francesco Capitelli,[e] and Cosimo Cardellicchio*[a]

Abstract: An experimental investigation of the enantioselective oxidation of aryl benzyl sulfides by *tert*-butyl hydroperoxide in the presence of a titanium/hydrobenzoin catalyst has shown that these sulfides are ideal substrates for this catalytic system, with negligible interference by the substituents on the aryl groups. A reaction mechanism based on DFT computations has been proposed. The DFT MPWB1K functional was used in the theoretical investigation to account for weak hydrogen-bonding and π interactions. The computed reaction profile explains the experimentally observed enantioselectivity, which is determined by the thermodynamics of the first phase of the reaction. A detailed discussion of the hydrogen-bonding and π interactions that drive the reaction along the observed stereochemical path is given.

Keywords: density functional calculations · enantioselectivity · oxidation · reaction mechanisms · titanium

Introduction

Enantiopure sulfoxides have been employed many times as starting materials in several asymmetric syntheses of natural and bioactive compounds.[1,2] Chiral non-racemic sulfoxides are prepared by two main strategies based upon the use of organometallic reagents[2–5] or the enantioselective oxidation of sulfides,[4–23] or by a suitable combination of these two approaches.[4,5] Because bioactive sulfoxides often bear moieties that are not compatible with organometallic procedures, chiral sulfinyl drugs are prepared industrially mostly by enantioselective oxidation,[7] as in the case of esomeprazole, one of the best-selling drugs.[8] Thus, recent interest in more efficient sulfide oxidation protocols is growing.[7] Although several enantioselective oxidation reactions have been reported,[6–23] the synthetic developments have not been accompanied by an increased understanding of the reaction mechanisms.

The most common oxidation protocols employ an achiral oxidant (hydroperoxides or peroxides) in the presence of chiral metal complexes. Many metals have been investigated, as reported in the pioneering work[9] of Modena and Kagan and their co-workers on titanium/diethyl tartrate complexes[8,9] and in other papers on different titanium complexes,[10–18] as well as on vanadium,[19–21] iron[22] or aluminium[23] catalysts, to cite the most frequently used metals.

Two main behaviour patterns were observed in these processes. 1) A sulfoxide with a high *ee* value was produced directly without the formation of significant amounts of sul-

[a] Prof. F. Naso, Dr. C. Cardellicchio
Dipartimento di Chimica and CNR ICCOM, Università di Bari
via Orabon 4, 70125 Bari (Italy)
Fax: (+39) 0805539596
E-mail: cardellicchio@ba.iccom.cnr.it

[b] Dr. M. A. M. Capozzi
Dipartimento di Scienze Agroambientali, Chimica e Difesa Vegetale
Università di Foggia, Via Napoli 25, 71100 Foggia (Italy)

[c] Prof. A. Bottoni, Dr. M. Calvaresi
Dipartimento di Chimica G. Ciamician, Università di Bologna
via Selmi 2, 40126 Bologna (Italy)
Fax: (+39) 0512099456
E-mail: andrea.bottoni@unibo.it

[d] Prof. V. Bertolasi
Dipartimento di Chimica and Centro di
Strutturistica Diffrattometrica
Università di Ferrara, via Borsari 46, 44100 Ferrara (Italy)

[e] Dr. F. Capitelli
CNR Istituto di Cristallografia
via Amendola 122/o, 70126 Bari (Italy)

Supporting information for this article is available on the WWW under http://dx.doi.org/10.1002/chem.200902110.

 © 2009 Wiley-VCH Verlag GmbH & Co. KGaA, Weinheim WILEY InterScience DISCOVER SOMETHING GREAT

fones.[8,9,12,14,15,17–19,21–23] 2) A sulfoxide with a lower *ee* value was obtained, but the enantiopurity could be increased if overoxidation to sulfone was allowed.[10–11,16,20] In fact, the acting catalyst can enhance the *ee* of the product sulfoxide by oxidising the minor enantiomer selectively.

In connection with our work on the application of carbanionic leaving groups to the synthesis of chiral sulfoxides,[4] we reported that enantiopure benzyl *p*-bromophenyl sulfoxide (**1b**) is a general and viable precursor of chiral non-racemic dialkyl sulfoxides provided that two subsequent substitution steps with alkyl Grignard reagents are carried out.[14] The precursor can be easily obtained in very high *ee* (> 98%) and in high isolated yield (85%) with the aid of a straightforward catalytic enantioselective oxidation of benzyl *p*-bromophenyl sulfide (**1a**) with *tert*-butyl hydroperoxide (TBHP) in the presence of a titanium/hydrobenzoin catalyst (Scheme 1).[14]

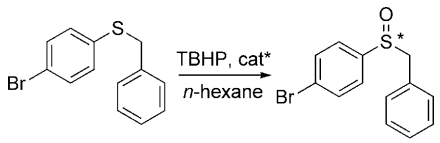

1a **1b**

cat* = Ti(O*i*Pr)$_4$/(*S*,*S*)- or (*R*,*R*)-hydrobenzoin

Scheme 1. Enantioselective oxidation of benzyl *p*-bromophenyl sulfide in the presence of a titanium/hydrobenzoin catalyst.

Both enantiomers of the hydrobenzoin ligand are cheap and easily available. The (*R*)-sulfoxide was obtained when (*S*,*S*)-hydrobenzoin was used, whereas the reaction afforded the (*S*)-sulfoxide in the presence of (*R*,*R*)-hydrobenzoin. Furthermore, the experimental procedure was insensitive to the presence of water, was effective at room temperature and could be performed in *n*-hexane,[14] a more environmentally benign solvent than the chlorinated solvents commonly used in other procedures. Moreover, with *n*-hexane the sulfoxide precipitated from the reaction medium and could easily be collected. A simple crystallisation step yielded the desired enantiopure material, thus allowing easy scale-up.[14]

Because this oxidation protocol is particularly efficient, we compared our results with other work[13,17,18] and looked for new applications.[15,16] High *ee* values and satisfactory yields were obtained in the oxidation of aryl β-ketosulfides (70–94% yields, 92 to >98% *ee*s).[15] Also with these sulfinyl compounds, the reaction gave (*R*)-sulfoxides when (*S*,*S*)-hydrobenzoin was used. The same protocol was applied to the oxidation of two alkyl esters of Sulindac sulfide, structurally related to an aryl methyl sulfide (95–96% *ee* values),[16] and an identical stereochemical outcome was again observed.[16] On the other hand, in this oxidation reaction, we observed a sulfone, a lower yield of the sulfoxide and an increase in the *ee* value due to a kinetic resolution process.[16] This pattern was confirmed by lower *ee* values when the formation of sulfone was inhibited by a shorter reaction time (4–6 h) or lower temperature (0 °C). Similar conditions, able to inhibit the formation of sulfone,[11] had been reported by Rosini an co-workers,[13] who oxidised various sulfides in the presence of a titanium/hydrobenzoin catalyst with the formation of the corresponding sulfoxides (55–73% yields, 22–80% *ee*s for aryl alkyl sulfoxides, 92 to >99% *ee*s for a few aryl benzyl sulfoxides). Going into detail, water was present in their protocol and 2 equiv of a different solution of TBHP were employed. Seto et al. used the titanium/hydrobenzoin catalyst to prepare a sulfoxide that was a precursor of an anti-HIV agent.[17] Note that a high *ee* (91%) and a satisfactory yield (71%) were obtained when a molecule similar to an aryl benzyl sulfide was oxidised at room temperature without the formation of appreciable quantities of sulfone. On the other hand, a slight structural variation of the sulfide caused a reduction in the yield and the *ee* (18%) of the sulfoxide product. Very recently, Jiang et al.[18] reported the oxidation of omeprazole-like sulfides with hydroperoxides in the presence of complexes formed between titanium and hydrobenzoins bearing different substituents on the aryl groups. Water was present. High yields (up to 92%) and *ee* values (up to 96% *ee*) were obtained for these heteroaryl molecules that resemble aryl benzyl sulfides.

From an overview of these results obtained under a variety of reaction conditions, the oxidation of aryl benzyl sulfides with hydroperoxides in the presence of a titanium/hydrobenzoin catalyst seemed to us to represent an ideal substrate/reagent/catalyst system for a detailed stereochemical and mechanistic investigation. With this aim, we decided to perform a systematic experimental investigation of the oxidation of a variety of aryl benzyl sulfides bearing different substituents on the aryl groups under the same reaction conditions. We carried out our experiments without inhibiting the possible formation of the sulfone to test if and when kinetic resolution was present. In addition, because the mechanistic details of titanium-catalysed oxidation have not been elucidated yet and, as far as we know, no accurate theoretical study is available in the literature, we investigated the potential energy surface of the reaction by using a reliable quantum mechanical DFT approach. To this purpose we employed a simple model system formed by a benzyl phenyl sulfide molecule reacting with *tert*-butyl hydroperoxide (TBHP) in the presence of a titanium/hydrobenzoin complex.

Results and Discussion

Reagents and reaction protocol: Aryl benzyl sulfides **2a**–**15a**[24–30] bearing different substituents were synthesised starting from the commercially available aryl thiols and the corresponding benzyl halides. As reported in Table 1, we chose sulfides bearing electron-withdrawing or -releasing substituents on the aryl groups. Furthermore, in principle, these groups could supply a further point of coordination for the titanium centre (for example, in the case of the methoxy moiety) and exert steric hindrance.

 © 2009 Wiley-VCH Verlag GmbH & Co. KGaA, Weinheim

Table 1. Enantioselective oxidation of aryl benzyl sulfides by TBHP in the presence of catalytic amounts of a titanium/(*S*,*S*)- or (*R*,*R*)-hydrobenzoin complex.

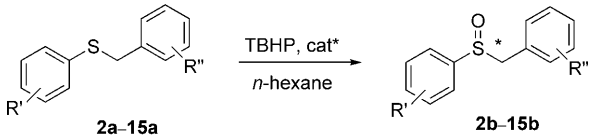

2a–15a **2b–15b**

cat* = Ti(O*i*Pr)$_4$/ (*S*,*S*)- or (*R*,*R*)-hydrobenzoin
Molar ratio: Ti(O*i*Pr)$_4$/hydrobenzoin/sulfide/TBHP 1:2:20:22

Entry	Sulfide	R′	R″	Ligand configuration	Sulfoxide	Yield [%][a]	*ee* [%][b]	ee_{cryst} [%][c]
1	**2a**	2-COOMe	H	(*S*,*S*)	(*R*)-**2b**[d]	77	91	>98
2	**3a**	2-Cl	H	(*S*,*S*)	(*R*)-**3b**[e]	92	95	
3	**4a**	4-NO_2	H	(*S*,*S*)	(*R*)-**4b**[d]	65[f]	>98	>98
4	**4a**	4-NO_2	H	(*R*,*R*)	(*S*)-**4b**[26]	38	>98	>98
5	**5a**	2-OMe	H	(*S*,*S*)	(*R*)-**5b**[d]	89	88	>98
6	**6a**	3-OMe	H	(*S*,*S*)	(*R*)-**6b**[d]	57	84	>98
7	**7a**	4-OMe	H	(*S*,*S*)	(*R*)-**7b**[33]	67	>98	>98
8	**7a**	4-OMe	H	(*R*,*R*)	(*S*)-**7b**[33]	65	>98	>98
9	**8a**	4-Br	2-NO_2	(*S*,*S*)	(*R*)-**8b**[d]	72	85	>98
10	**9a**	4-Br	4-NO_2	(*S*,*S*)	(*R*)-**9b**[d]	71	>98	>98
11	**10a**	4-Br	2-OMe	(*S*,*S*)	(*R*)-**10b**[d]	68	>98	>98
12	**11a**	4-Br	3-OMe	(*S*,*S*)	(*R*)-**11b**[d]	37	81	>98
13	**12a**	4-Br	4-OMe	(*S*,*S*)	(*R*)-**12b**[e]	65	>98	>98
14	**13a**	4-Br	3-Cl	(*S*,*S*)	(*R*)-**13b**[d]	66	97	97
15	**14a**	4-Br	2,4-Cl_2	(*S*,*S*)	(*R*)-**14b**[d]	82[g]	>98	>98
16	**14a**	4-Br	2,4-Cl_2	(*S*,*S*)	(*R*)-**14b**[d]	47[h]	85	
17	**15a**	4-OMe	4-OMe	(*S*,*S*)	(*R*)-**15b**[e]	72	>98	>98

[a] Isolated yields. [b] The *ee* values were measured by HPLC (see text) before crystallization. [c] The ee_{cryst} values were measured by HPLC after crystallization. [d] The absolute configurations of the sulfoxides were established by X-Ray analysis (see text). [e] This configuration was attributed on the basis of our empirical rule (see text). [f] The reaction was performed in a 20:3 mixture of *n*-hexane/CCl_4 due to the high insolubility of sulfide **3a** in pure *n*-hexane. [g] The corresponding sulfone was also present in a yield of 14%. [h] This reaction was performed at 0°C for 7 h.

The oxidation reactions of **2a–15a** to obtain sulfoxides **2b–15b**[26,31–33] were performed in *n*-hexane (Table 1). In fact, the enantioselectivities of these reactions are higher in apolar solvents[13–18] such as carbon tetrachloride or *n*-hexane, but we preferred to avoid the use of toxic chlorinated solvents. Sometimes, this environmental choice had a drawback because the reaction was slower in *n*-hexane. As a consequence, a certain amount of the starting sulfide remained in the mixture after two days and the yield decreased in comparison with the same reaction performed in carbon tetrachloride.

The reactions were performed on a 1 mmol scale with 1.1 mmol of oxidant at room temperature for two days in the presence of 0.05 mmol of a 1:2 titanium/hydrobenzoin catalyst. Many of the chiral aryl benzyl sulfoxides that were produced precipitated from the reaction medium but, instead of collecting them as in our previous work,[14] we preferred to subject the whole reaction mixture to chromatography in order to measure the *ee* values of the sulfoxides before crystallisation (81 to >98%). In fact, as reported in Table 1, the enantiomeric purity of these sulfoxides were usually higher after crystallisation (*ee* >98%). In principle, this protocol could be subjected to experimental improvements, but we were interested in performing all the reactions under the same conditions.

Experimental results: After screening the structures (Table 1, entries 1–17) we were in a position to confirm that the enantioselective oxidation of aryl benzyl sulfides with *tert*-butyl hydroperoxide in the presence of a titanium/hydrobenzoin catalyst is extremely efficient from a synthetic point of view. In fact, very often it was possible to obtain in an easy and straightforward manner the corresponding sulfoxides **2b–15b** with very high enantiomeric purity (>98% after crystallisation). The yields were satisfactory (57–92% with two exceptions), even when *n*-hexane was used as the solvent.

Most of the reactions were performed by using (*S*,*S*)-hydrobenzoin as the ligand for titanium, but two of them (Table 1, entries 4 and 8) were repeated with the (*R*,*R*)-hydrobenzoin to obtain the enantiomeric sulfoxide. In the cases of sulfoxides **2b**, **4b–6b**, **8b–11b**, **13b** and **14b**, the absolute configuration at the sulfur atom was established by X-ray analysis. When (*S*,*S*)-hydrobenzoin was used as the titanium ligand, the sulfur atom of these sulfoxides had the *R* configuration, thus confirming our empirical rule.[14–16] Note that the four molecules that were not found suitable for X-ray analysis were compound **3b**, which is an oil, and compounds **7b**, **12b** and **15b**, in which a *para*-methoxy group is present in one or both of the aryl groups of the molecule.

The tridimensional crystal structure is the result of many interactions, the most important being hydrogen-bonding between the benzyl methylene group and the sulfinyl oxygen atom. Furthermore, other contributions from the heteroatoms (for example, halogen-bonding[34]) were present. In the crystal structure, the aryl groups of the sulfoxides **2b**, **5b**, **9b**, **11b** and **13b** are arranged in a gauche conformation (values of the dihedral angle (aryl carbon)-(methylene carbon)-sulfur-(aryl′ carbon) are in the range of 52–65°). On the other hand, in compounds **4b**, **6b**, **8b**, **10b** and **14b**, the aryl groups are arranged in an antiperiplanar conformation (dihedral angle values in the range 166–179°). More details are presented in the Supporting Information.

The stereochemical picture that emerged from this oxidation is extremely interesting. As reported in Table 1, very high *ee* values (>95%) were obtained for nine out of the fourteen sulfoxides (Table 1, entries 2–4, 7, 8, 10, 11, 13–15 and 17), and *ee* values in the range 81–91% were measured for the remaining ones.

 © 2009 Wiley-VCH Verlag GmbH & Co. KGaA, Weinheim

In particular, as far as the substitution on the aryl group bonded to the sulfur atom is concerned (Table 1, entries 1–8), a slight but significant decrease in the *ee* values (84–88%) was observed when a methoxy group was present in the *ortho* or *meta* position (entries 5 and 6). Because a higher *ee* value (95%) was obtained after the introduction of a non-coordinating *ortho*-chloro substituent (Table 1, entry 2), this effect could be due to the interference of a coordinating group close to the metal centre. On the other hand, the same moiety in a different position (Table 1, entries 7 and 8) did not particularly affect the enantioselectivity (>98% *ee*).

As far as the substitution on the benzyl aryl group is concerned (Table 1, entries 9–17), excellent enantioselectivities were obtained (97 to >98% *ee* values) with two exceptions. The first is with the *ortho*-nitro moiety on the benzyl aryl group (Table 1, entry 9, *ee* 85%). The second is with the *meta*-methoxy group (Table 1, entry 12). In this case, not only the *ee* value decreased (81% *ee*, which is the lowest value of the whole investigation), but the yield also dropped to 37% with a very large amount of sulfide **11a** remaining unreacted. The decrease in both yield and enantioselectivity could be ascribed to the presence of a coordinating group because the oxidation of sulfide **13a** (Table 1, entry 14), in which the chlorine atom is present in the same *meta*-position, yielded an usually high *ee* (97%) and a satisfactory yield (66%).

Another exception was the formation of a certain amount (14%) of the corresponding sulfone from the oxidation of sulfide **14a** (Table 1, entry 15). The reaction was repeated at 0°C for 7 h to test whether kinetic resolution was present (Table 1, entry 16). Under these conditions, a 53:47 mixture of sulfide **14a**/sulfoxide **14b** was obtained with no trace of the sulfone, the *ee* of **14b** being 82%. Because sulfoxide **14b** was produced in an enantiopure form (entry 15), only in this particular case is a certain amount of kinetic resolution present.

From the results presented in Table 1 and in a previous paper,[14] with some exceptions, aryl benzyl sulfides seem to be appropriate substrates for enantioselective oxidation in the presence of a titanium/hydrobenzoin catalyst because high *ee* values were always measured. Slight decreases in enantioselectivity could be ascribed to the local interference of some groups placed in certain positions.

Mechanistic investigations: With these results in hand, we tried to envisage a reaction mechanism that could explain the observed reaction selectivity. As outlined in the Introduction section, the mechanism for the metal-catalysed enantioselective oxidation of sulfides is still far from being understood. A mechanistic scheme was suggested for vanadium catalysts,[21] but nothing similar has been reported for active titanium species, even though titanium was the first metal that was proposed for these reactions[9] and a huge amount of literature relating to its use has been published in more than 25 years.[6,7]

The proposal of a plausible reaction mechanism encountered serious problems,[35–37] the most significant being the experimental evidence for a fast exchange of titanium ligands in solution[35] and the formation of supramolecular assemblies. It has been demonstrated that the complexes formed between titanium and tartrates[36] and between titanium and BINOL[14,37] yield intricate patterns when observed by spectroscopic techniques. However, when we recorded the ^{1}H NMR spectrum[14] of the complex obtained from a 1:2 mixture of titanium isopropoxide and hydrobenzoin, we observed a very simple pattern arising from a titanium complex in which only the hydrobenzoin was bound to the metal with the original isopropoxide moiety free in solution. The different behaviour characterising the titanium/hydrobenzoin complex with respect to the other catalysts led us to hypothesise that a less complicated reaction mechanism could be operating.

Following our hypothesis, the starting tetrahedral Ti(hydrobenzoin)$_2$ species, which originates from the initial 1:2 mixture of titanium isopropoxide and hydrobenzoin, first undergoes oxidative addition of the sulfide and then of the oxidant. This would lead to the formation of an octahedral assembly that is expected to be stable enough to transfer the oxygen atom from the hydroperoxide moiety to the sulfur atom, in accord with the experimental results, that is, lead to the formation of the (*R*)- or (*S*)-sulfoxide when (*S*,*S*)- or (*R*,*R*)-hydrobenzoin is used, respectively. Furthermore, within our mechanistic hypothesis, aryl benzyl sulfides should be the best fitting substrates.

Computational details and choice of model: Because most of the experimentally investigated aryl substituents do not significantly affect the enantioselectivity of the reaction, we have used in our calculations the simplest (prototype) model system, a benzyl phenyl sulfide molecule, which reacts with *tert*-butyl hydroperoxide (TBHP) in the presence of a titanium/hydrobenzoin complex. In particular, we chose (*S*,*S*)-hydrobenzoin and considered the two possible reaction pathways leading to the (*S*)- or (*R*)-sulfoxide, this last configuration being in agreement with the experimental results.

Owing to the presence of aryl groups in the ligands and in the substrate, it is reasonable to believe that interactions involving the aryl π systems should be taken into account, as was assumed by other workers.[13] Thus, an appropriate method for their description must be chosen. It is well known that this class of interactions cannot be correctly treated at the DFT level of theory because the most popular functionals (for instance, B3LYP) are inaccurate for interactions in which medium-range correlation effects are dominant.[38]

In fact, π–π interactions are satisfactorily described by the MP2 method but, given the size of the model system used here (47 heavy atoms and 36 hydrogen atoms), MP2 computations require too much CPU time for practical and extensive use. However, a new hybrid functional (denoted as MPWB1K), which is capable of treating medium-range correlation effects, has recently been proposed.[39] This func-

 © 2009 Wiley-VCH Verlag GmbH & Co. KGaA, Weinheim

tional has been demonstrated to provide a good estimate of π–π interactions and reaction energies[40,41] using reasonable amounts of CPU time.

Thus, all the DFT computations reported in this paper were carried out with the Gaussian 03 software package[42] using the MPWB1K[39] functional and the DZVP basis set.[43] The DZVP basis set is a local spin density (LSD) optimised basis set of double-zeta quality that includes polarisation functions and is suitable for describing weak hydrogen bonds and π interactions such as those occurring in the system investigated herein. The transition vector of the various transition states has been analysed by frequency computations. Furthermore, because an apolar solvent (*n*-hexane) was used in our experiments, on the basis of our experience, we believe that gas-phase computations can satisfactorily emulate the experimental conditions.

Computational results: The corresponding energy profile for the oxidation of the benzyl phenyl sulfide molecule by *tert*-butyl hydroperoxide (TBHP) in the presence of a titanium-(hydrobenzoin)$_2$ complex is reported in Figure 1 and schematic representations of the structures of the most important critical points are reported in Figures 2–4 and Figures 1S and 2S of the Supporting Information. The asymptotic limit (AL) in Figure 1 is represented by the titanium-(hydrobenzoin)$_2$ tetrahedral complex (see Figure 1S), a benzyl phenyl sulfide substrate molecule and a TBHP molecule at infinite distance (that is, the reactants).

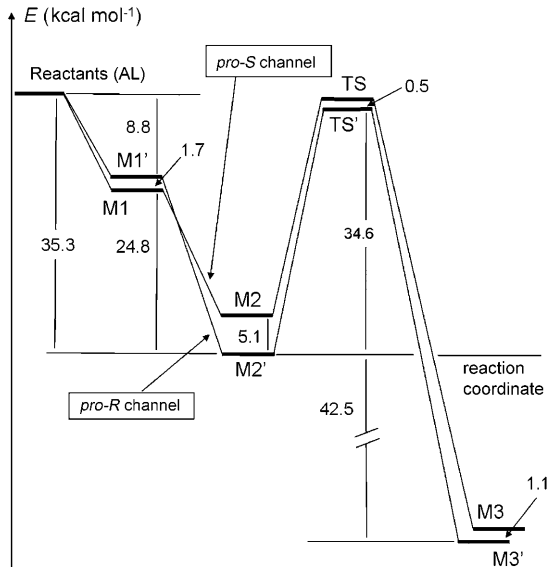

Figure 1. Computed energy profile for the enantioselective TBHP oxidation of benzyl phenyl sulfide in the presence of a titanium/(*S*,*S*)-hydrobenzoin catalyst.

The substrate molecule can adopt two different orientations to interact with the tetrahedral complex involving the (*S*,*S*)-hydrobenzoin enantiomer. The two approaches lead to the formation of two pentacoordinated titanium species M1 and M1′ without overcoming any barrier. Because M1 and M1′ afford final products with the *S* and *R* configuration at the sulfur atom, respectively, they can be denoted as *pro-S* and *pro-R* compounds (see Figure 2). The energy difference between these two species is 1.7 kcal mol^{-1} and the one with lower energy is the *pro-S* species M1, which is 10.5 kcal mol^{-1} below the AL.

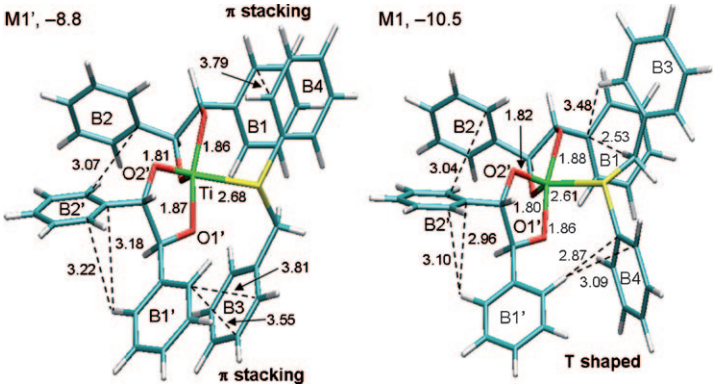

Figure 2. Schematic representation of the structures of the two diastereomeric titanium pentacoordinate adducts M1′ and M1 (bond lengths in Å). Energy values (kcal mol^{-1}) are relative to the AL.

Inspection of Figure 2 shows that as the sulfide enters into the metal coordination sphere the original Ti(hydrobenzoin)$_2$ tetrahedral structure becomes distorted and the two five-membered rings (CCO1TiO2 and CCO1′TiO2′) are now bent in the opposite direction with respect to the approaching line of the sulfide. The Ti–O bond lengths are quite similar in the two intermediates and the newly formed Ti–S bond is shorter in M1 (2.61 Å) than in M1′ (2.68 Å).

The two pentacoordinated titanium complexes are characterised by a number of interactions involving the phenyl rings of the substrate and those of the two hydrobenzoin ligands. However, the nature of these interactions is rather different in the two cases. In M1′ π-stacking interactions are evident between each phenyl ring of the sulfide (B3 and B4) and one of the two phenyl rings of each hydrobenzoin moiety (B1 and B1′, respectively). The two rings of each pair lie in approximately parallel planes, but do not form the well-known "sandwich" structure. The two planes are displaced to give a structural arrangement that has been demonstrated to provide more effective π–π stabilisation.[44–46] Typical distances between the most effectively interacting carbon atoms of the two rings are in the range 3.6–3.9 Å and are reported in Figure 2.

In M1 the orientation of the substrate is reversed compared to M1′, and this leads in the final product to the opposite configuration at the sulfur atom (the *S* configuration). The result of the different substrate arrangement is a shorter Ti–S distance and the appearance in M1 of a T-shaped configuration[45–47] involving the ring-pair B1′/B4. In the T-shaped structure the plane of the hydrobenzoin phenyl ring B1′ is approximately orthogonal (but tilted) with respect to

 © 2009 Wiley-VCH Verlag GmbH & Co. KGaA, Weinheim

the plane of the substrate ring B4. This particular arrangement (tilted T-shaped) is known to be more stabilising than "parallel-displaced" and "sandwich" structures (π stacking) because, in addition to dispersion forces and quadrupole–quadrupole electrostatic effects, further stabilisation occurs due to hydrogen-bonding contributions.[47] In this case, one C–H bond of B1′ interacts with the π-electron cloud of B4: the (phenyl-B1′)C–H···C(phenyl-B4) distances that feature the tilted T-shaped interaction are in the range of 2.9–3.6 Å (specific values are reported in Figure 2).

It is interesting to examine the relative arrangements of B1 and B3 in M1. The methylene group placed between the sulfur and benzene makes it difficult in this case to achieve a T-shaped structure such as that observed for the B1′/B4 pair. However, one of the C–H bonds of the methylene group points towards B1 and gives rise to a non-negligible hydrogen interaction. This is evidenced by the (methylene)C–H···C(phenyl-B1) distances: the shortest computed value is 2.53 Å, which indicates a non-negligible interaction of the C–H bond with the π-electron cloud of B1. Even if this C–H···π interaction is less stabilising than a full benzene dimer interaction (1.5 versus 2.5 kcal mol^{-1}),[47] the two rings remain close enough to believe that some stabilising effects associated with π–π aromatic interactions remain active (for instance, dispersion forces and quadrupole–quadrupole effects) and must contribute to the C–H···π stabilisation. Furthermore, a comparison between the two structures of Figure 2 shows that in the two species the relative positions and distances between B1′, B2′ and B2 do not change significantly and thus the interactions involving these three rings should not affect the relative stabilities of M1 and M1′.

In conclusion, the shorter Ti–S distance observed in M1 and the stabilisation associated with the T-shaped structure and C–H···π interactions explain the lower energy of M1 compared with M1′.

The subsequent step involves the reaction of *tert*-butyl hydroperoxide with the pentacoordinated complexes. In principle, we could consider a deprotonated hydroperoxide reagent. However, in this case the charged hydroperoxide that results from the deprotonation forms a η^2 complex with the titanium atom and determines the expulsion of the sulfide from the metal coordination sphere. The system obtained in this way is stable and cannot lead to any oxidation product. Thus, it seems reasonable to consider the addition of neutral TBHP. We found that this leads to the formation of two new species (M2 from M1 and M2′ from M1′, see Figure 3) in which the metal adopts an octahedral arrangement. The difference in energy between M2 and M2′ is 5.1 kcal mol^{-1} and the favoured structure is now M2′, that is, the complex leading to the experimentally observed *R* configuration of the final product.

It is evident from Figure 3 that the nature of the interactions significantly changes on passing from M1 to M2. Although in M1 T-shaped interactions characterise the B1′/B4 pair, in M2 these two rings are too far away for an effective stabilisation. More interesting is the arrangement of the two rings B1 and B3. A stabilising interaction (methylene)C–H···C(phenyl-B1) (similar to that described for M1) can be recognised (a (methylene)C–H···C(phenyl-B1) distance of 2.64 Å reflects the relative positions of methylene and B1). Furthermore, there is a significant hydrogen bond involving the O4–H group and the O1′ oxygen, the O4–H···O1′ distance being 1.84 Å.

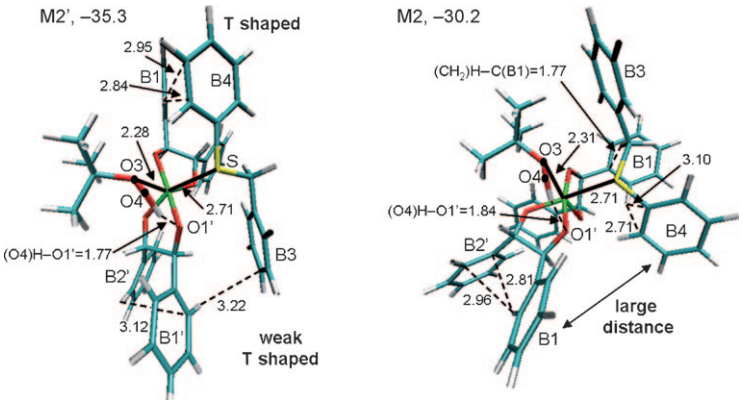

Figure 3. Schematic representation of the structures of the two diastereomeric titanium octahedral adducts M2′ and M2 (bond lengths in Å). Energy values (kcal mol^{-1}) are relative to the AL.

Because in M2′ B3 and B1′ are tilted compared with their positions in M1′, π-stacking interactions become impossible. However, the relative arrangement of the B3 and B1′ planes (these are oblique and displaced one to the other) leads to a sort of weakly bound T-shaped structure characterised by the interaction of one of the C–H bonds of B1′ with the π-electron cloud of B3: the shortest (phenyl-B1′)C–H···C(phenyl-B3) distance is 3.22 Å.

The B1–B4 π-stacking interactions found in M1′ also disappear in M2′. However, in this case, B1 is approximately orthogonal to B4 and originates a stabilising tilted T-shaped configuration.[45–47] The interaction of one of the C–H bonds of B1 with the π-electron cloud of B4 is evident from Figure 3(left): the shortest (phenyl-B1)C–H···C(phenyl-B4) distances that reveal this tilted T-shaped interaction are 2.84 and 2.95 Å (as shown in Figure 3 left). A further interesting aspect found in M2′ is the O4–H···O1′ hydrogen bond, which is stronger than in M2, the O4–H···O1′ distance now being 1.77 Å.

Because the Ti–S and Ti–O3 distances are almost identical in M2 and M2′, it is reasonable to believe that the B1–B4 T-shaped structure, the additional (even weak) interactions involving B1′ and B3 and the O4–H···O1′ hydrogen bond are the key factors that determine the lower energy of M2′ compared with M2.

The computed energy difference between M2 and M2′ indicates that under thermodynamic conditions such as those governing the first part of the reaction, the latter species should form almost exclusively. The thermodynamic equilibration requires a barrier of 30.2 kcal mol^{-1} to be overcome (needed by M2 to break the Ti–O and Ti–S bonds and allow the substrate to reorientate to afford M2′). This amount of energy is almost identical to the activation barri-

 © 2009 Wiley-VCH Verlag GmbH & Co. KGaA, Weinheim

er needed to achieve the subsequent transition state and is, thus, available under the experimental conditions used for the reaction.

The two transition states TS and TS′ (see Figure 4) leading to the final sulfoxide products from M2 and M2′, respectively, were located. These are almost degenerate, their energy difference being 0.5 kcal mol^{-1}, with TS′ more stable than TS.

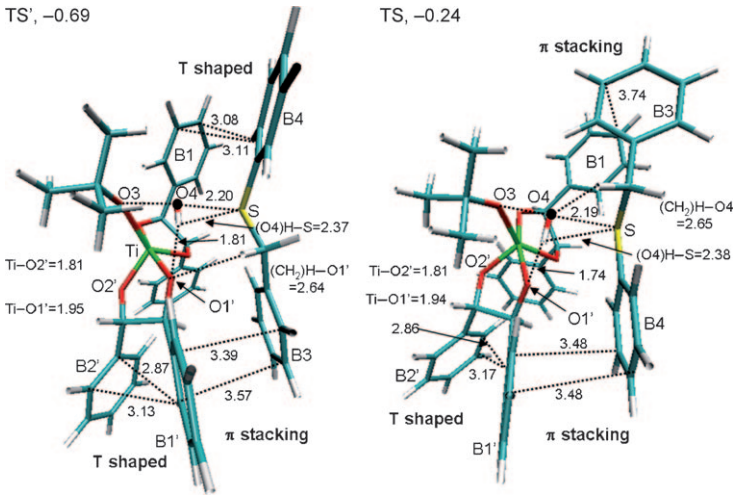

Figure 4. Schematic representation of the structures of the two transition states TS′ and TS (bond lengths in Å). Energy values (kcal mol^{-1}) are relative to the AL.

In TS and TS′ a new bond is forming between the sulfur atom and the oxygen atom O4 of the hydroperoxide molecule (the incipient S–O4 bond is 2.20 and 2.19 Å in TS′ and TS, respectively). Simultaneously, the hydrogen atom migrates from O4 to O1′ causing a lengthening of the Ti–O1′ bond (the (O4)H–O1′ and Ti–O1′ distances are 1.81 and 1.95 Å in TS′ and 1.74 and 1.94 Å in TS, respectively, whereas the corresponding value for Ti–O2′ is 1.81 Å in both cases). In both TS′ and TS B1′ interacts with the adjacent phenyl ring of the substrate (B3 in TS′ and B4 in TS) in a parallel-displaced arrangement (this corresponds to a weak π-stacking interaction in which the C···C bond lengths of the two rings are larger than 3.4 Å). Also, B1′ interacts with B2′ to form a T-shaped structure that is almost identical in the two transition states. A further interesting feature is the H(O4)···S hydrogen bond which assists the proton transfer. The strength of this interaction is almost identical in TS′ and TS, the H(O4)···S distances being 2.37 and 2.38 Å, respectively. A hydrogen bond between the methylene group of the sulfide and the O1′ atom can be identified in TS′ ((CH$_2$)H···O1′distance = 2.64 Å). This interaction is replaced in TS by an equivalent hydrogen bond involving O4 ((CH$_2$)H···O4 distance = 2.65 Å). In fact, the two structures TS′ and TS are very similar, except for the arrangement of the two rings B1 and B4 in TS′ and B1and B3 in TS. B1 and B3 are approximately planar (displaced π-stacking), whereas the relative positions of B1 and B4 resemble a T-shaped structure. All these structural features detected in TS′ and TS explain their almost negligible energy difference.

The two transition states lead to the final product complexes M3 (from TS along the *pro-S* pathway) and M3′ (from TS′ along the *pro-R* pathway), which are the precursors of the enantiomer benzyl phenyl sulfoxides. A schematic representation of the two complexes is given in Figure 2S of the Supporting Information. As found for TS′ and TS, M3′ is more stable than M3, the energy difference being 1.1 kcal mol^{-1}. Again, a complex interplay of many factors, such as π–π aromatic and C–H···π interactions determine the relative energies of the two product adducts. A shorter Ti–O4 distance in M3′ (2.20 Å) compared with M3 (2.25 Å) certainly contributes to the stabilisation of the former species.

However, this aspect is not particularly important because the final product complexes are very low in energy compared with the previously discussed critical points: M3′ is 42.5 kcal mol^{-1} lower than M2′ and 77.8 kcal mol^{-1} below the AL. Thus, the relative populations of M3 and M3′ (the two products with opposite configuration at the sulfur) cannot be determined by their relative energies. Under the experimental conditions used for this reaction, it is very unlikely that thermodynamic equilibration occurs because the conversion of M3 to M3′ would require a barrier of 76.5 kcal mol^{-1} to be overcome (this amount of energy is required to achieve the transition state TS).

It is reasonable to believe that the observed *ee* (which requires that M3′ is much more populated than M3) is determined by the energetics of the first phase of the reaction and the corresponding kinetics. Because, as previously discussed, M2′ is formed almost exclusively during the first reaction phase and the two transition states are almost degenerate, the most likely pathway to complete the process is that involving TS′ leading to M3′ (the adduct with the *R* configuration at the sulfur atom). The required activation barrier is 34.6 kcal mol^{-1}, a value that is very similar to the amount of energy necessary for the reverse reaction to yield the reactants. Finally, the decomposition of M3′ will produce the desired sulfoxide.

Conclusions

In the work presented in this paper, it has been shown experimentally that high *ee* values and satisfactory yields are obtained in the enantioselective preparation of synthetically important aryl benzyl sulfoxides by enantioselective oxidation by TBHP in the presence of a titanium/hydrobenzoin catalyst. The origin of this high enantioselectivity has been explained by a mechanistic scheme that has been studied theoretically at the DFT level of theory using the recently proposed MPWB1K functional. This functional can provide a reliable description of medium-range correlation effects that play a key role in determining the relative stabilities of the various critical points on the potential surface. A simple (prototype) model system, formed by a benzyl phenyl sul-

 © 2009 Wiley-VCH Verlag GmbH & Co. KGaA, Weinheim

fide molecule reacting with *tert*-butyl hydroperoxide (TBHP) in the presence of a titanium/(*S*,*S*)-hydrobenzoin complex, has been used. Two reaction pathways (*pro-R* and *pro-S*) corresponding to the two possible approaching orientations of sulfide to the Ti(hydrobenzoin)$_2$ complex and leading to the (*R*)- and (*S*)-sulfoxides, respectively, have been considered.

The two reaction channels (*pro-S*: AL→M1→M2→TS; *pro-R*: AL→M1′→M2′→TS′) are characterised by a first phase that affords the two preliminary intermediates M2 and M2′ (octahedral adducts) with M2′ more stable than M2 by 5.1 kcal mol^{-1}. Our computations demonstrated that T-shaped structures, which are present only in M2′, are the key factors determining the greater stability of this intermediate. Because the reverse reaction from M2 to the reactants requires a barrier of 30.2 kcal mol^{-1} to be overcome (an amount of energy almost identical to that necessary to reach the subsequent transition state) it seems reasonable to believe that thermodynamic equilibration occurs and M2′ forms almost exclusively. From M2′ the system "naturally" evolves to the final product adduct M3′ (second phase), which can release the experimentally observed sulfoxide with the *R* configuration at the sulfur atom. Thus, the thermodynamics of the first phase of the process (and the consequent dominant population of M2′) is the key factor that determines the high enantioselectivity.

Experimental Section

Chemicals were purchased from Sigma–Aldrich or Alfa-Aesar and were used as received. *n*-Hexane employed in the enantioselective oxidation protocol was distilled from 4 Å molecular sieves prior to use. NMR spectra were recorded on a Bruker AM500 spectrometer. HPLC were performed on an Agilent 1100 chromatograph, equipped with a DAD detector. Elemental analyses were performed on a Carlo Erba CHNS-O EA1108 Elemental Analyzer. Sulfides **2a**–**15a** were synthesised by a standard reaction between the corresponding sodium arylthiolates and benzyl bromides.

Methyl (2-benzylthio)benzoate (2a): M.p. 65–66 °C (ethanol) (lit.:[24] m.p. 56–58 °C).

Benzyl 2-chlorophenyl sulfide (3a): Kugelrohr oven temp. 130–132 °C; $p = 0.01$ mbar (lit.:[25] b.p. 159–160 °C, $p = 3$ torr).

Benzyl 4-nitrophenyl sulfide (4a): M.p. 118–120 °C (ethanol) (lit.:[26] m.p. 120–122 °C).

(*R*)-Benzyl 2-methoxyphenyl sulfide (5a):[27] Kugelrohr oven temp. 140–142 °C; $p = 0.01$ mbar.

Benzyl 3-methoxyphenyl sulfide (6a):[27] Kugelrohr oven temp. 118–121 °C; $p = 0.01$ mbar.

Benzyl 4-methoxyphenyl sulfide (7a):[27] Kugelrohr oven temp. 123–125 °C; $p = 0.01$ mbar.

4-Bromophenyl 2-nitrobenzyl sulfide (8a): M.p. 50–51 °C (ethanol); ^{1}H NMR (500 MHz, $CDCl_3$, 25 °C, TMS): $\delta = 7.99$ (dd, ^4J(H, H) = 1.5, ^3J(H, H) = 8.0 Hz, 1H; H_{Ar}), 7.46 (dt, ^4J(H, H) = 1.5, ^3J(H, H) = 7.6 Hz, 1H; H_{Ar}), 7.40 (ddd, ^4J(H, H) = 1.5, ^3J(H, H) = 7.6, ^3J(H, H) = 8.0 Hz, 1H; H_{Ar}), 7.38–7.34 (m, 2H; H_{Ar}), 7.24 (dd, ^4J(H, H) = 1.5, ^3J(H, H) = 7.6 Hz, 1H; H_{Ar}), 7.16–7.12 (m, 2H; H_{Ar}), 4.41 ppm (s, 2H; CH_2). ^{13}C NMR (125 MHz, $CDCl_3$, 25 °C, TMS): $\delta = 133.8$ (C_{Ar}), 133.3 (C_{Ar}), 133.1 (C_{Ar}), 132.0 (C_{Ar}), 131.8 (C_{Ar}), 128.4 (C_{Ar}), 125.4 (C_{Ar}), 121.6 (C_{Ar}), 37.3 ppm (CH_2); elemental analysis calcd (%) for $C_{13}H_{10}BrNO_2S$: C 48.16, H 3.11, N 4.32; found: C 48.43, H 3.48, N 4.40.

4-Bromophenyl 4-nitrobenzyl sulfide (9a): M.p. 102–104 °C (ethanol) (lit.:[28] m.p. 104–105 °C).

4-Bromophenyl 2-methoxybenzyl sulfide (10a): Kugelrohr oven temp. 136–138 °C; $p = 0.01$ mbar; ^{1}H NMR (500 MHz, $CDCl_3$, 25 °C, TMS): $\delta =$ 7.38–7.34 (m, 2H; H_{Ar}), 7.24 (ddd, ^4J(H, H) = 1.6, ^3J(H, H) = 7.5, ^3J(H, H) = 8.2 Hz, 1H; H_{Ar}), 7.19–7.16 (m, 3H; H_{Ar}), 6.89–6.85 (m, 2H; H_{Ar}), 4.12 (s, 2H; CH_2), 3.82 ppm (s, 3H; OCH_3); ^{13}C NMR (125 MHz, $CDCl_3$, 25 °C, TMS): $\delta = 136.0$ (C_{Ar}), 131.7 (C_{Ar}), 131.5 (C_{Ar}), 130.1 (C_{Ar}), 128.7 (C_{Ar}), 125.3 (C_{Ar}), 120.4 (C_{Ar}), 120.0 (C_{Ar}), 110.5 (C_{Ar}), 55.4 (OCH_3), 33.4 ppm (CH_2); elemental analysis calcd (%) for $C_{14}H_{13}BrOS$: C 54.38, H 4.24; found: C 54.40, H 4.15.

4-Bromophenyl 3-methoxybenzyl sulfide (11a): Kugelrohr oven temp. 138–140 °C; $p = 0.01$ mbar; ^{1}H NMR (500 MHz, $CDCl_3$, 25 °C, TMS): $\delta =$ 7.38–7.35 (m, 2H; H_{Ar}), 7.20 (t, ^3J(H, H) = 7.8 Hz, 1H; H_{Ar}), 7.17–7.14 (m, 2H; H_{Ar}), 6.87–6.85 (m, 1H; H_{Ar}), 6.83–6.82 (m, 1H; H_{Ar}), 6.81–6.77 (m, 1H; H_{Ar}), 4.06 (s, 2H; CH_2), 3.77 ppm (s, 3H; OCH_3); ^{13}C NMR (125 MHz, $CDCl_3$, 25 °C, TMS): $\delta = 159.7$ (C_{Ar}), 138.5 (C_{Ar}), 135.4 (C_{Ar}), 131.8 (C_{Ar}), 131.4 (C_{Ar}), 129.5 (C_{Ar}), 121.1 (C_{Ar}), 114.2 (C_{Ar}), 112.9 (C_{Ar}), 55.2 (OCH_3), 39.0 ppm (CH_2); elemental analysis calcd (%) for $C_{14}H_{13}BrOS$: C 54.38, H 4.24; found: C 54.05, H 4.30.

4-Bromophenyl 4-methoxybenzyl sulfide (12a): M.p. 99–101 °C (ethanol) (lit.:[29] m.p. 100.5–101 °C)

4-Bromophenyl 3-chlorobenzyl sulfide (13a): Kugelrohr oven temp. 160–162 °C; $p = 0.01$ mbar; ^{1}H NMR (500 MHz, $CDCl_3$, 25 °C, TMS): $\delta = 7.39$–7.36 (m, 2H; H_{Ar}), 7.28–7.26 (m, 1H; H_{Ar}), 7.22–7.19 (m, 2H; H_{Ar}), 7.16–7.11 (m, 3H; H_{Ar}), 4.03 ppm (s, 2H; CH_2); ^{13}C NMR (125 MHz, $CDCl_3$, 25 °C, TMS): $\delta = 139.2$ (C_{Ar}), 134.7 (C_{Ar}), 134.3 (C_{Ar}), 132.0 (C_{Ar}), 131.8 (C_{Ar}), 129.7 (C_{Ar}), 128.8 (C_{Ar}), 127.5 (C_{Ar}), 126.9 (C_{Ar}), 120.8 (C_{Ar}), 38.7 ppm (CH_2); elemental analysis calcd (%) for $C_{13}H_{10}BrClS$: C 49.78, H 3.21; found: C 49.70, H 3.55.

4-Bromophenyl 2,4-dichlorobenzyl sulfide (14a): Kugelrohr oven temp. 162–165 °C, $p = 0.01$ mbar; ^{1}H NMR (500 MHz, $CDCl_3$, 25 °C, TMS): $\delta =$ 7.39–7.36 (m, 3H; H_{Ar}), 7.18–7.10 (m, 4H; H_{Ar}), 4.12 ppm (s, 2H; CH_2); ^{13}C NMR (125 MHz, $CDCl_3$, 25 °C, TMS): $\delta = 134.7$ (C_{Ar}), 134.2 (C_{Ar}), 133.8 (C_{Ar}), 133.6 (C_{Ar}), 132.6 (C_{Ar}), 132.0 (C_{Ar}), 131.3 (C_{Ar}), 129.5 (C_{Ar}), 127.1 (C_{Ar}), 121.2 (C_{Ar}), 36.6 ppm (CH_2); elemental analysis calcd (%) for $C_{13}H_9BrCl_2S$: C 44.86, H 2.61; found: C 44.89, H 2.93.

4-Methoxyphenyl 4-methoxybenzyl sulfide (15a): M.p. 82–84 °C (ethanol) (lit.:[30] 87–88 °C).

Racemic sulfoxides **2b**–**15b** (used in the setting up of the chiral HPLC separation) were synthesised by standard *m*-chloroperbenzoic acid (MCPBA) oxidation. Enantioenriched sulfoxides **2b**–**15b** were produced according to our protocol[14] by TBHP oxidation in *n*-hexane in the presence of 5 mol-% of the titanium/hydrobenzoin catalyst.

X-Ray data were collected at 293 K by using a single-crystal X-ray diffractometer. Data were corrected for Lorentzian and polarisation effects as well as for absorption effects (**8b**–**11b**, **13b** and **14b**).[48] The structures were solved by direct methods using SIR97[49] and refined by a full-matrix least-squares technique based on F^2 (SHELXL-97).[50] In all the refinements, the non-hydrogen atoms were refined with anisotropic thermal parameters. The hydrogen atoms were located through difference Fourier maps and refined isotropically with the exception of **8b**, **9b**, **13b** and **14b**, for which the hydrogen atoms were placed in idealised positions riding on their attached atoms (C–H_{Ar} 0.93 Å, C–H_{Alk} 0.97 Å, $U_{iso}(H) = 1.2U_{iso}(C)$). Geometrical calculations were performed by using PARST.[51]

The unit cell parameters, data collection and refinement are reported in the Supporting Information. CCDC-720081 (**2b**), −720082 (**4b**), −720083 (**5b**), −720084 (**6b**), −720085 (**8b**), −720086 (**9b**), −720087 (**10b**), −720088 (**11b**), −720089 (**13b**) and −720090 (**14b**) contain the supplementary crystallographic data for this paper. These data can be obtained free of charge from The Cambridge Crystallographic Data Centre via www.ccdc.cam.ac.uk/data_request/cif.

Methyl (*R*)-(2-benzylsulfinyl)benzoate (2b): M.p. 151–152 °C (*n*-hexane/ethanol 9:1) (lit.:[31] racemic m.p. 118–120 °C); $[\alpha]_D^{25} = +433.7$ ($c = 0.8$ in $CHCl_3$). The *ee* value was measured by HPLC (column: Chiralcel OD-H; eluent: *n*-hexane/isopropanol 70:30).

© 2009 Wiley-VCH Verlag GmbH & Co. KGaA, Weinheim

(*R*)-Benzyl 2-chlorophenyl sulfoxide (3b):[32] $[\alpha]_D^{25}=+397.1$ ($c=1$ in $CHCl_3$). The *ee* value was measured by HPLC (column: Chiralcel OB-H; eluent: *n*-hexane/isopropanol 90:10).

(*R*)-Benzyl 4-nitrophenyl sulfoxide (4b): M.p. 196–198 °C (ethanol/ethyl acetate 15:3); $[\alpha]_D^{25}=+114.6$ ($c=0.9$ in $CHCl_3$).

(*S*)-Benzyl 4-nitrophenyl sulfoxide (4b): M.p. 198–199 °C (ethanol/ethyl acetate 15:3) (lit.:[26] m.p. 179–181); $[\alpha]_D^{25}=-115.5$ ($c=1.1$ in $CHCl_3$) and $[\alpha]_D^{25}=-259.9$ ($c=0.5$ in acetone) (lit.:[26] $[\alpha]_D^{25}=-163.6$ ($c=0.93$ in acetone)). The *ee* value was measured by HPLC (column: Chiralcel OD-H; eluent: *n*-hexane/isopropanol 70:30).

(*R*)-Benzyl 2-methoxyphenyl sulfoxide (5b): M.p. 60–61 °C (*n*-hexane/isopropanol 9:1), $[\alpha]_D^{25}=+510.3$ ($c=1$ in $CHCl_3$) (lit.:[33] +351 ($c=0.32$ in $CHCl_3$) for a sulfoxide with 81 % *ee*). The *ee* value was measured by HPLC (column: Chiralcel OD-H; eluent: *n*-hexane/isopropanol 95:5).

(*R*)-Benzyl 3-methoxyphenyl sulfoxide (6b): M.p. 86–87 °C (*n*-hexane/acetone 19:1); $[\alpha]_D^{25}=+78.6$ ($c=0.9$ in $CHCl_3$) and $[\alpha]_D^{25}=+198.5$ ($c=0.5$ in acetone) (lit.:[33] +73.5 ($c=0.17$ in acetone)) for a sulfoxide with 69 % *ee*). The *ee* value was measured by HPLC (column: Chiralcel OD-H; eluent: *n*-hexane/isopropanol 90:10).

(*R*)-Benzyl 4-methoxyphenyl sulfoxide (7b): M.p. 136–137 °C (*n*-hexane/ethanol 15:1); $[\alpha]_D^{25}=+57.8$ ($c=1.2$ in $CHCl_3$) (lit.:[33] +31.9 ($c=0.28$ in $CHCl_3$) for a sulfoxide with 44 % *ee*).

(*S*)-Benzyl 4-methoxyphenyl sulfoxide (7b): M.p. 135–136 °C (*n*-hexane/ethanol 15:1); $[\alpha]_D^{25}=-59.7$ ($c=0.6$ in $CHCl_3$). The *ee* value was measured by HPLC (column: Chiralcel OD-H; eluent: *n*-hexane/isopropanol 90:10).

(*R*)-4-Bromophenyl 2-nitrobenzyl sulfoxide (8b): M.p. 97–98 °C (*n*-hexane/ethanol 9:1); $[\alpha]_D^{25}=+203.4$ ($c=0.9$ in $CHCl_3$); ^{1}H NMR (500 MHz, $CDCl_3$, 25 °C, TMS): $\delta=8.04$ (dd, ^4J(H, H) = 1.4, ^3J(H, H) = 8.1 Hz, 1H; H_{Ar}), 7.59–7.55 (m, 2H; H_{Ar}), 7.54 (dt, ^4J(H, H) = 1.4, ^3J(H, H) = 7.5 Hz, 1H; H_{Ar}), 7.47 (ddd, ^4J(H, H) = 1.5, ^3J(H, H) = 7.5, ^3J(H, H) = 8.1 Hz, 1H; H_{Ar}), 7.38–7.35 (m, 2H; H_{Ar}), 7.25 (dd, ^4J(H, H) = 1.5, ^3J(H, H) = 7.5 Hz, 1H; H_{Ar}), 4.61 (d, ^2J(H, H) = 12.6 Hz, 1H; CH_2), 4.13 ppm (d, ^2J(H, H) = 12.6 Hz, 1H; CH_2); ^{13}C NMR (125 MHz, $CDCl_3$, 25 °C, TMS): $\delta=142.1$ (C_{Ar}), 134.1 (C_{Ar}), 133.6 (C_{Ar}), 132.4 (C_{Ar}), 129.7 (C_{Ar}), 126.0 (C_{Ar}), 125.6 (C_{Ar}), 125.5 (C_{Ar}), 125.4 (C_{Ar}), 61.8 ppm (CH_2); elemental analysis calcd (%) for $C_{13}H_{10}BrNO_3S$: C 45.90, H 2.96, N 4.12; found: C 46.18, H 2.83, N 4.21. The *ee* value was measured by HPLC (column: Whelk O1; eluent: *n*-hexane/isopropanol 70:30).

(*R*)-4-Bromophenyl 4-nitrobenzyl sulfoxide (9b): M.p. 153–154 °C (*n*-hexane/ethanol 7:3); $[\alpha]_D^{25}=+279.3$ ($c=0.9$ in $CHCl_3$); ^{1}H NMR (500 MHz, $CDCl_3$, 25 °C, TMS): $\delta=8.14$–8.11 (m, 2H; H_{Ar}), 7.61–7.58 (m, 2H; H_{Ar}), 7.23–7.20 (m, 2H; H_{Ar}), 7.15–7.11 (m, 2H; H_{Ar}), 4.20 (d, ^2J(H, H) = 12.8 Hz, 1H; CH_2), 3.99 ppm (d, ^2J(H, H) = 12.8 Hz, 1H; CH_2); ^{13}C NMR (125 MHz, $CDCl_3$, 25 °C, TMS): $\delta=147.8$ (C_{Ar}), 140.9 (C_{Ar}), 135.6 (C_{Ar}), 132.4 (C_{Ar}), 131.3 (C_{Ar}), 126.1 (C_{Ar}), 125.7 (C_{Ar}), 123.4 (C_{Ar}), 61.7 ppm (CH_2); elemental analysis calcd (%) for $C_{13}H_{10}BrNO_3S$: C 45.90, H 2.96, N 4.12; found: C 45.71, H 2.63, N 4.45. The *ee* value was measured by HPLC (column: Whelk O1; eluent: *n*-hexane/isopropanol/methylene chloride 70:20:10).

(*R*)-4-Bromophenyl 2-methoxybenzyl sulfoxide (10b): M.p. 64–66 °C (*n*-hexane/ethanol 9:1); $[\alpha]_D^{25}=-58.0$ ($c=1.1$ in $CHCl_3$); ^{1}H NMR (500 MHz, $CDCl_3$, 25 °C, TMS): $\delta=7.55$–7.52 (m, 2H; H_{Ar}), 7.29 (ddd, ^4J(H, H) = 1.7, ^3J(H, H) = 7.4, ^3J(H, H) = 8.2 Hz, 1H; H_{Ar}), 7.26–7.23 (m, 2H; H_{Ar}), 6.96 (dd, ^4J(H, H) = 1.7, ^3J(H, H) = 7.4 Hz, 1H; H_{Ar}), 6.87 (dt, ^4J(H, H) = 1.0, ^3J(H, H) = 7.4 Hz, 1H; H_{Ar}), 6.79 (dd, ^4J(H, H) = 1.0, ^3J(H, H) = 8.2 Hz, 1H; H_{Ar}), 4.24 (d, ^2J(H, H) = 12.2 Hz, 1H; CH_2), 4.02 (d, ^2J(H, H) = 12.2 Hz, 1H; CH_2), 3.64 ppm (s, 3H; OCH_3); ^{13}C NMR (125 MHz, $CDCl_3$, 25 °C, TMS): $\delta=157.5$ (C_{Ar}), 132.2 (C_{Ar}), 131.7 (C_{Ar}), 131.5 (C_{Ar}), 130.1 (C_{Ar}), 126.1 (C_{Ar}), 125.4 (C_{Ar}), 120.4 (C_{Ar}), 117.3 (C_{Ar}), 110.2 (C_{Ar}), 58.4 (CH_2), 55.2 ppm (OCH_3); elemental analysis calcd (%) for $C_{14}H_{13}BrO_2S$: C 51.70, H 4.03; found: C 51.99, H 4.38. The *ee* value was measured by HPLC (column: Chiralcel OD-H; eluent: *n*-hexane/isopropanol 95:5).

(*R*)-4-Bromophenyl 3-methoxybenzyl sulfoxide (11b): M.p. 104–105 °C (*n*-hexane/acetone 9:1); $[\alpha]_D^{25}=+50.0$ ($c=1$ in $CHCl_3$); ^{1}H NMR (500 MHz, $CDCl_3$, 25 °C, TMS): $\delta=7.58$–7.55 (m, 2H; H_{Ar}), 7.26–7.23 (m, 2H; H_{Ar}), 7.18 (dd, ^3J(H, H) = 7.5, ^3J(H, H) = 8.2 Hz, 1H; H_{Ar}), 6.84 (ddd, ^4J(H, H) = 0.9, ^4J(H, H) = 2.6, ^3J(H, H) = 8.2 Hz, 1H; H_{Ar}), 6.57 (ddd, ^4J(H, H) = 0.9, ^4J(H, H) = 1.4, ^3J(H, H) = 7.5 Hz, 1H; H_{Ar}), 6.49 (dd, ^4J(H, H) = 1.4, ^4J(H, H) = 2.6 Hz, 1H; H_{Ar}), 4.09 (d, ^2J(H, H) = 12.6 Hz, 1H; CH_2), 3.93 (d, ^2J(H, H) = 12.6 Hz, 1H; CH_2), 3.72 ppm (s, 3H; OCH_3); ^{13}C NMR (125 MHz, $CDCl_3$, 25 °C, TMS): $\delta=159.6$ (C_{Ar}), 132.0 (C_{Ar}), 130.0 (C_{Ar}), 129.6 (C_{Ar}), 126.1 (C_{Ar}), 125.7 (C_{Ar}), 122.6 (C_{Ar}), 115.4 (C_{Ar}), 114.4 (C_{Ar}), 63.6 (CH_2), 55.2 ppm (OCH_3); elemental analysis calcd (%) for $C_{14}H_{13}BrO_2S$: C 51.70, H 4.03; found C 51.56, H 4.21. The *ee* value was measured by HPLC (column: Chiralcel OD-H; eluent: *n*-hexane/isopropanol 90:10).

(*R*)-4-Bromophenyl 4-methoxybenzyl sulfoxide (12b): M.p. 173–175 °C (*n*-hexane/ethanol 8:2); $[\alpha]_D^{25}=+70.1$ ($c=0.9$ in $CHCl_3$); ^{1}H NMR (500 MHz, $CDCl_3$, 25 °C, TMS): $\delta=7.58$–7.54 (m, 2H; H_{Ar}), 7.23–7.19 (m, 2H; H_{Ar}), 6.90–6.86 (m, 2H; H_{Ar}), 6.81–6.77 (m, 2H; H_{Ar}), 4.04 (d, ^2J(H, H) = 12.7 Hz, 1H; CH_2), 3.94 (d, ^2J(H, H) = 12.7 Hz, 1H; CH_2), 3.79 ppm (s, 3H; OCH_3); ^{13}C NMR (125 MHz, $CDCl_3$, 25 °C, TMS): $\delta=159.7$ (C_{Ar}), 141.9 (C_{Ar}), 132.0 (C_{Ar}), 131.6 (C_{Ar}), 126.1 (C_{Ar}), 125.5 (C_{Ar}), 120.4 (C_{Ar}), 114.0 (C_{Ar}), 62.7 (CH_2), 55.3 ppm (OCH_3); elemental analysis calcd (%) for $C_{14}H_{13}BrO_2S$: C 51.70, H 4.03; found C 51.50, H 3.99. The *ee* value was measured by HPLC (column: Chiralcel OD-H; eluent: *n*-hexane/isopropanol 90:10).

(*R*)-4-Bromophenyl 3-chlorobenzyl sulfoxide (13b): M.p. 116–117 °C (*n*-hexane/acetone 8:2); $[\alpha]_D^{25}=+103.6$ ($c=0.8$ in $CHCl_3$); ^{1}H NMR (500 MHz, $CDCl_3$, 25 °C, TMS): $\delta=7.61$–7.56 (m, 2H; H_{Ar}), 7.31–7.18 (m, 4H; H_{Ar}), 6.97–6.94 (m, 1H; H_{Ar}), 6.89–6.85 (m, 1H; H_{Ar}), 3.98 ppm (s, 2H; CH_2); ^{13}C NMR (125 MHz, $CDCl_3$, 25 °C, TMS): $\delta=141.5$ (C_{Ar}), 134.4 (C_{Ar}), 132.2 (C_{Ar}), 130.6 (C_{Ar}), 130.3 (C_{Ar}), 129.7 (C_{Ar}), 128.6 (C_{Ar}), 128.5 (C_{Ar}), 125.9 (C_{Ar}), 62.7 ppm (CH_2); elemental analysis calcd (%) for $C_{13}H_{10}BrClOS$: C 47.37, H 3.06; found: C 47.66, H 3.22. The *ee* value was measured by HPLC (column: Whelk O1; eluent: *n*-hexane/isopropanol 70:30).

(*R*)-4-Bromophenyl 2,4-dichlorobenzyl sulfoxide (14b): M.p. 117–118 °C (*n*-hexane/acetone 8:2); $[\alpha]_D^{25}=+76.2$ ($c=0.9$ in $CHCl_3$); ^{1}H NMR (500 MHz, $CDCl_3$, 25 °C, TMS): $\delta=7.63$–7.57 (m, 2H; H_{Ar}), 7.39 (d, ^4J(H, H) = 2.0 Hz, 1H; H_{Ar}), 7.35–7.30 (m, 2H; H_{Ar}), 7.20 (dd, ^4J(H, H) = 2.0, ^3J(H, H) = 8.2 Hz, 1H; H_{Ar}), 7.07 (d, ^3J(H, H) = 8.2 Hz, 1H; H_{Ar}), 4.18 (d, ^2J(H, H) = 12.8 Hz, 1H; CH_2), 4.14 ppm (d, ^2J(H, H) = 12.8 Hz, 1H; CH_2); ^{13}C NMR (125 MHz, $CDCl_3$, 25 °C, TMS): $\delta=135.5$ (C_{Ar}), 135.4 (C_{Ar}), 133.4 (C_{Ar}), 132.3 (C_{Ar}), 129.5 (C_{Ar}), 127.3 (C_{Ar}), 126.1 (C_{Ar}), 126.0 (C_{Ar}), 125.9 (C_{Ar}), 60.6 ppm (CH_2); elemental analysis calcd (%) for $C_{13}H_9BrCl_2OS$: C 42.89, H 2.49; found C 42.90, H 2.60. The *ee* value was measured by HPLC (column: Chiralcel OD-H; eluent: *n*-hexane/isopropanol 70:30).

(*R*)-4-Methoxyphenyl 4-methoxybenzyl sulfoxide (15b): M.p. 159–160 °C (*n*-hexane/ethanol 9:1); $[\alpha]_D^{25}=+31.3$ ($c=0.4$ in $CHCl_3$); ^{1}H NMR (500 MHz, $CDCl_3$, 25 °C, TMS): $\delta=7.32$–7.29 (m, 2H; H_{Ar}), 6.95–6.91 (m, 2H; H_{Ar}), 6.90–6.86 (m, 2H; H_{Ar}), 6.80–6.76 (m, 2H; H_{Ar}), 4.06 (d, ^2J(H, H) = 12.7 Hz, 1H; CH_2), 3.93 (d, ^2J(H, H) = 12.7 Hz, 1H; CH_2), 3.84 (s, 3H; OCH_3), 3.79 ppm (s, 3H; OCH_3); ^{13}C NMR (125 MHz, $CDCl_3$, 25 °C, TMS): $\delta=162.0$ (C_{Ar}), 159.6 (C_{Ar}), 131.6 (C_{Ar}), 130.1 (C_{Ar}), 129.9 (C_{Ar}), 126.5 (C_{Ar}), 114.3 (C_{Ar}), 113.9 (C_{Ar}), 62.9 (CH_2), 55.5 (OCH_3), 55.2 ppm (OCH_3); elemental analysis calcd (%) for $C_{15}H_{16}O_3S$: C 65.19, H 5.84; found: C 65.49, H 6.05. The *ee* value was measured by HPLC (column: Chiralcel OD-H; eluent: *n*-hexane/isopropanol 90:10).

Acknowledgements

This work was financially supported, in part, by the MIUR Rome (PRIN Project: Stereoselezione in sintesi organica. Metodologie e applicazioni) and by the University of Bari. We thank Luca Nigro, Caterina Centrone, Antonio Spadaro and Elena Lorusso for preliminary oxidation experiments, and Prof. Marcello Colapietro (Dipartimento di Chimica, Università "La Sapienza", Roma, Italy) and Giuseppe Chita (CNR, Istituto di Cristallografia, Bari, Italy) for X-ray data collection.

 © 2009 Wiley-VCH Verlag GmbH & Co. KGaA, Weinheim

[1] G. H. Posner in *The Chemistry of Sulphones and Sulphoxides* (Eds.: S. Patai, Z. Rappoport, C. Stirling), Wiley, New York, **1988**, pp. 823–849; G. Solladié in *Advanced Asymmetric Synthesis* (Ed.: G. R. Stephenson), Chapman and Hall, London, **1996**, pp. 60–92; M. C. Carreño, *Chem. Rev.* **1995**, *95*, 1717–1760.
[2] I. Fernandez, N. Khiar, *Chem. Rev.* **2003**, *103*, 3651–3705.
[3] J. L. Garcia Ruano, C. Alemparte, M. T. Aranda, M. M. Zarzuelo, *Org. Lett.* **2003**, *5*, 75–78; Z. Han, D. Krishnamurthy, P. Grover, H. S. Wilkinson, Q. K. Fang, X. Su, Z.-H. Lu, D. Magiera, C. H. Senanayake, *Angew. Chem.* **2003**, *115*, 2078–2081; *Angew. Chem. Int. Ed.* **2003**, *42*, 2032–2035.
[4] M. A. M. Capozzi, C. Cardellicchio, F. Naso, *Eur. J. Org. Chem.* **2004**, 1855–1863.
[5] D. A. Cogan, G. Liu, K. Kim, B. J. Backes, J. A. Ellman, *J. Am. Chem. Soc.* **1998**, *120*, 8011–8019.
[6] C. Bolm, K. Muñiz, J. P. Hildebrand in *Comprehensive Asymmetric Catalysis*, (Eds.: E. N. Jacobsen, A. Pfalz, H. Yamamoto), Springer, Berlin, **1999**, pp. 697–710.
[7] J. Legros, J. R. Dehli, C. Bolm, *Adv. Synth. Catal.* **2005**, *347*, 19–31.
[8] H. Cotton, T. Elebring, M. Larsson, L. Li, H. Sorensen, S. von Unge, *Tetrahedron: Asymmetry* **2000**, *11*, 3819–3825.
[9] P. Pitchen, E. Duñach, M. N. Deshmukh, H. B. Kagan, *J. Am. Chem. Soc.* **1984**, *106*, 8188–8193; S. H. Zhao, O. Samuel, H. B. Kagan, *Tetrahedron* **1987**, *43*, 5135–5144; F. Di Furia, G. Modena, R. Seraglia, *Synthesis* **1984**, 325–327; O. Bortolini, F. Di Furia, G. Licini, G. Modena, M. Rossi, *Tetrahedron Lett.* **1986**, *27*, 6257–6260.
[10] N. Komatsu, M. Hashizume, T. Sugita, S. Uemura, *J. Org. Chem.* **1993**, *58*, 4529–4533; N. Komatsu, M. Hashizume, T. Sugita, S. Uemura, *J. Org. Chem.* **1993**, *58*, 7624–7626.
[11] X. Jia, X. Li, L. Xu, Y. Li, Q. Shi, T. T.-L. Au-Yeung, C. W. Yip, X. Yao, A. S. C. Chan, *Adv. Synth. Catal.* **2004**, *346*, 723–726.
[12] M. A. M. Capozzi, C. Cardellicchio, G. Fracchiolla, F. Naso, P. Tortorella, *J. Am. Chem. Soc.* **1999**, *121*, 4708–4709; M. A. M. Capozzi, C. Cardellicchio, F. Naso, *Tetrahedron: Asymmetry* **2004**, *15*, 1471–1476.
[13] M. I. Donnoli, S. Superchi, C. Rosini, *J. Org. Chem.* **1998**, *63*, 9392–9395; S. Superchi, P. Scafato, L. Restaino, C. Rosini, *Chirality* **2008**, *20*, 592–596.
[14] M. A. M. Capozzi, C. Cardellicchio, F. Naso, V. Rosito, *J. Org. Chem.* **2002**, *67*, 7289–7294.
[15] C. Cardellicchio, O. Hassan Omar, F. Naso, M. A. M. Capozzi, F. Capitelli, V. Bertolasi, *Tetrahedron: Asymmetry* **2006**, *17*, 223–229.
[16] F. Naso, C. Cardellicchio, F. Affortunato, M. A. M. Capozzi, *Tetrahedron: Asymmetry* **2006**, *17*, 3226–3229.
[17] M. Seto, N. Miyamoto, K. Aikawa, Y. Aramaki, N. Kanzai, Y. Iizawa, M. Baba, M. Shiraishi, *Bioorg. Med. Chem.* **2005**, *13*, 363–386.
[18] B. Jiang, X.-L. Zhao, J.-J. Dong, W.-J. Wang, *Eur. J. Org. Chem.* **2009**, 987–991.
[19] C. Bolm, *Coord. Chem. Rev.* **2003**, *237*, 245–256.
[20] C. Drago, L. Caggiano, R. F. W. Jackson, *Angew. Chem.* **2005**, *117*, 7387–7389; *Angew. Chem. Int. Ed.* **2005**, *44*, 7221–7223.
[21] K. P. Bryliakov, E. P. Talsi, T. Kühn, C. Bolm, *New J. Chem.* **2003**, *27*, 609–614; D. Balcells, F. Maseras, A. Lledós, *J. Org. Chem.* **2003**, *68*, 4265–4274; D. Balcells, F. Maseras, G. Ujaque, *J. Am. Chem. Soc.* **2005**, *127*, 3624–3634.
[22] J. Legros, C. Bolm, *Chem. Eur. J.* **2005**, *11*, 1086–1092; A. Korte, J. Legros, C. Bolm, *Synlett* **2004**, 2397–2399.
[23] T. Yamaguchi, K. Matsumoto, B. Saito, T. Katsuki, *Angew. Chem.* **2007**, *119*, 4813–4815; *Angew. Chem. Int. Ed.* **2007**, *46*, 4729–4731; K. Matsumoto, T. Yamaguchi, T. Katsuki, *Chem. Commun.* **2008**, 1704–1706.
[24] J.-F. Bonfanti, D. Craig, *Tetrahedron Lett.* **2005**, *46*, 3719–3723.
[25] S. V. Kessar, U. K. Nadir, P. Singh, Y. P. Gupta, *Tetrahedron* **1978**, *34*, 449–451.
[26] M. I. Donnoli, S. Superchi, C. Rosini, *Enantiomer* **2000**, *5*, 181–188.
[27] J. Ham, I. Yang, H. Kang, *J. Org. Chem.* **2004**, *69*, 3236–3239.
[28] J. Degani, A. Tundo, *Ann. Chim.* **1961**, *51*, 543–549.
[29] C. Wang, A. S. Batsanov, M. R. Bryce, I. Sage, *Synthesis* **2003**, 2089–2095.
[30] A. Krawczyk, J. T. Wrobel, *Rocz. Chemii* **1977**, *51*, 285–290.
[31] H. Kwart, H. Omura, *J. Am. Chem. Soc.* **1971**, *93*, 7250–7256.
[32] R. C. Gadwood, I. M. Mallick, A. J. DeWinter, *J. Org. Chem.* **1987**, *52*, 774–782.
[33] P. Kelly, S. E. Lawrence, A. R. Maguire, *Synlett* **2007**, 1501–1506.
[34] P. Metrangolo, F. Meyer, T. Pilati, G. Resnati, G. Terraneo, *Angew. Chem.* **2008**, *120*, 6206–6220; *Angew. Chem. Int. Ed.* **2008**, *47*, 6114–6127; F: Naso, C. Cardellicchio, M. A. M. Capozzi, F. Capitelli, V. Bertolasi, *New J. Chem.* **2006**, *30*, 1782–1789.
[35] Y.-T. Wu, Y.-C. Ho, C.-C. Lin, H.-M. Gau, *Inorg. Chem.* **1996**, *35*, 5948–5952.
[36] P. G. Potvin, B. G. Fieldhouse, *Tetrahedron: Asymmetry* **1999**, *10*, 1661–1672.
[37] G. Pescitelli, L. Di Bari, P. Salvadori, *Organometallics* **2004**, *23*, 4223–4229; G. Pescitelli, L. Di Bari, P. Salvadori, *J. Organomet. Chem.* **2006**, *691*, 2311–2318.
[38] Y. Zhao, D. G. Truhlar, *Acc. Chem. Res.* **2008**, *41*, 157–167.
[39] Y. Zhao, D. G. Truhlar, *J. Phys. Chem. A* **2004**, *108*, 6908–6918.
[40] Y. Zhao, D. G. Truhlar, *J. Phys. Chem. A* **2005**, *109*, 5656–5667.
[41] Y. Zhao, O. Tishchenko, D. G. Truhlar, *J. Phys. Chem. B* **2005**, *109*, 19046–19051.
[42] Gaussian 03, Revision A.1, M. J. Frisch, G. W. Trucks, H. B. Schlegel, G. E. Scuseria, M. A. Robb, J. R. Cheeseman, J. A. Montgomery, Jr., T. Vreven, K. N. Kudin, J. C. Burant, J. M. Millam, S. S. Iyengar, J. Tomasi, V. Barone, B. Mennucci, M. Cossi, G. Scalmani, N. Rega, G. A. Petersson, H. Nakatsuji, M. Hada, M. Ehara, K. Toyota, R. Fukuda, J. Hasegawa, M. Ishida, T. Nakajima, Y. Honda, O. Kitao, H. Nakai, M. Klene, X. Li, J. E. Knox, H. P. Hratchin, J. B. Cross, C. Adamo, J. Jaramillo, R. Gomperts, R. E. Stratmann, O. Yazyev, A. J. Austin, R. Cammi, C. Pomelli, J. W. Ochterski, P. Y. Ayala, K. Morokuma, G. A. Voth, P. Salvador, J. J. Dannenberg, V. G. Zakrzewski, S. Dapprich, A. D. Daniels, M. C. Strain, O. Farkas, D. K. Malik, A. D. Rabuck, K. Raghavachari, J. B. Foresman, J. V. Ortiz, Q. Cui, A. G. Baboul, S. Clifford, J. Cioslowski, B. B. Stefanov, G. Liu, A. Liashenko, P. Piskorz, I. Komaromi, R. L. Martin, D. J. Fox, T. Keith, A. Al-Lahan, C. Y. Peng, A. Nanayakkara, M. Challacombe, P. M. W. Gill, B. Johnson, W. Chen, M. W. Wong, C. Gonzalez, J. A. Pople, Gaussian Inc., Pittsburg, PA, **2003**.
[43] N. Godbout, D. R. Salahub, J. Andzelm, E. Wimmer, *Can. J. Chem.* **1992**, *70*, 560–571.
[44] E. A. Meyer, R. K. Castellano, F. Diederich, *Angew. Chem.* **2003**, *115*, 1244–1287; *Angew. Chem. Int. Ed.* **2003**, *42*, 1210–1250.
[45] T. Janowski, P. Pulay, *Chem. Phys. Lett.* **2007**, *447*, 27–32.
[46] M. Pitoňa'k, P. Neogra'dy, J. Rëza'č, P. Jurečka, M. Urban, P. Hobza, *J. Chem. Theory Comput.* **2008**, *4*, 1829–1834.
[47] M. O. Sinnokrot, C. D. Sherill, *J. Phys. Chem. A* **2006**, *110*, 10656–10668.
[48] SADABS, Absorption Correction Program, G. M. Sheldrick, University of Göttingen, Göttingen, **1996**; R. H. Blessing, *Acta Crystallogr. Sect. A* **1995**, *51*, 33–38; Oxford Diffraction, CrysAlis CCD and CrysAlis RED, Oxford Diffraction Ltd, Abingdon, **2006**.
[49] A. Altomare, M. C. Burla, M. Camalli, G. L. Cascarano, C. Giacovazzo, A. Guagliardi, A. G. G. Moliterni, G. Polidori, R. Spagna, *J. Appl. Crystallogr.* **1999**, *32*, 115–119.
[50] SHELXL-97. Program for the Refinement of Crystal Structures, G. M. Sheldrick, University of Göttingen, Göttingen, **1997**.
[51] M. Nardelli, *Appl. Crystallogr.* **1995**, *28*, 659.

Received: July 29, 2009
Published online: November 11, 2009

 © 2009 Wiley-VCH Verlag GmbH & Co. KGaA, Weinheim